

# An Efficient Algorithm for Multimodal Medical Image Fusion based on Feature Selection and PCA Using DTCWT (FSPCA-DTCWT)

Type of article: Original Article

Abdallah Bengueddoudj, Zoubeida Messali

Department of Electrical Engineering, University of BordjBouArreridj, BordjBouArreridj,  
Algeria

## Abstract:

**Background:** During the two past decades, medical image fusion has become an essential part of modern medicine due to the availability of numerous imaging modalities (MRI, CT, SPECT, etc.). This paper presents a new medical image fusion algorithm based on DTCWT and uses different fusion rules in order to obtain a new image which contains more information than any of the input images.

**Methods:** A new image fusion algorithm improves the visual quality of the fused image, based on feature selection and Principal Component Analysis (PCA) in the Dual-Tree Complex Wavelet Transform (DTCWT) domain. It is called Feature Selection with Principal Component Analysis and Dual-Tree Complex Wavelet Transform (FSPCA-DTCWT). Using different fusion rules in a single algorithm result in correctly reconstructed image (fused image), this combination will produce a new technique, which employs the advantages of each method separately. The DTCWT presents good directionality since it considers the edge information in six directions and provides approximate shift invariant. The main goal of PCA is to extract the most significant characteristics (represented by the wavelet coefficients) in order to improve the spatial resolution. The proposed algorithm fuses the detailed wavelet coefficients of input images using features selection rule

**Results:** Several experiments have been conducted over different sets of multimodal medical images such as CT/MRI, MRA/T1-MRI. However, due to pages-limit on a paper, only results of three sets have been presented. The FSPCA-DTCWT algorithm is compared to recent fusion methods presented in the literature (eight methods) in terms of visual quality and quantitatively using well-known fusion performance metrics (five metrics). Results showed that the proposed algorithm outperforms the existing ones regarding visual and quantitative evaluations.

**Conclusion:** This paper focuses on image fusion of medical images obtained from different modalities. A novel image fusion algorithm based on DTCWT to merge multimodal medical images, has been proposed. Experiments have been performed over two different sets of multimodal medical images. The results show that the proposed fusion method significantly outperforms the recent fusion techniques reported in the literature.

**Keywords:** Multimodal medical images; Image fusion; DTCWT; PCA; Feature selection

**Corresponding author:** Abdallah Bengueddoudj, Department of Electrical Engineering, University of BordjBouArreridj, BordjBouArreridj, Algeria

Email: [beng.abdallah@hotmail.com](mailto:beng.abdallah@hotmail.com)

Received: June 30, 2017, Accepted: December 12, 2017, English editing: February 25, 2018, Published: March 19, 2018.

Screened by iThenticate. ©2017KNOWLEDGE KINGDOM PUBLISHING.

## 1. INTRODUCTION

Nowadays, medical image fusion has become a useful and important tool in surgical interventions and diagnostics. The principle of image fusion is based on the combination of information from multiple images obtained from different sensors into a single image [1]. The objective of image fusion is to preserve the most important features of each source images. The latter one, are captured using different biomedical detectors, which are used to extract complementary information about human tissues. Different medical imaging modalities such as Magnetic Resonance Image (MRI), Computed Tomography (CT), Positron Emission Tomography (PET) and Single Photon Emission Tomography (SPECT) can localize the abnormal masses and give an easy overview of the anatomic

detail. Imaging methods have their own characteristics and limitations. As an example, CT images take excellent picture of bones and other dense structures whereas MR images are perfectly describing information about soft tissues. Similarly, the MR images have higher spatial resolution than the PET images, which provides anatomical information without functional activity. Hence, we can conclude that these complementarities may be combined in order to generate an image that can offer more information than any of the individual source images. For example, medical PET/CT imaging is used for cancer detection, SPECT/CT fusion [2] in abdominal studies, and MRI/PET for brain tumor detection. Similarly, MRI/CT and PET/SPECT imaging [3] contribute to planning surgical procedure. In this case, the purpose of medical image fusion is to obtain an image with high spatial resolution and also integrates both functional and anatomical information.

In the present work, we have proposed a novel architecture with a hybrid algorithm based on DTCWT, the developed fusion algorithm (FSPCA-DTCWT) integrates different fusion rules to combine the wavelet coefficients of multimodal medical image fusion method. FSPCA-DTCWT is compared to recent fusion methods presented in the literature in terms of visual quality and quantitatively using the well-known fusion performance metrics. The rest of this paper is organized as follows: Image fusion literature is discussed in Section 2. Properties of DTCWT are described in Section 3. Section 4 explains the proposed fusion algorithm (FSPCA-DTCWT). Experimental results and performance evaluations are given in Sections 5. Finally, conclusions of the work are given in Section 6.

## 2. Procedure for Background and Literature

Many fusion methods have been proposed in the literature. These methods can be performed at three different levels depending on the stage at which the combination mechanism takes place, namely: pixel level, feature level and decision level [5]. Fusion at pixel-level is performed directly on the values derived from the pixels of the source images on a pixel-by-pixel basis to generate a single fused image. Feature level image fusion is one level higher than the pixel-level image fusion. Methods belong to this level represent used region based fusion scheme. The input images are divided (segmented) into regions, and various region properties can be calculated and used to determine which features from each original image are used in the fused image. In general, the fusion process at any level should always preserve all possible important information existed in the source images; on the other hand, the fusion process should be able to generate an image without introducing any artefacts, noise, unpredicted characteristic or loss of information [6].

Several pixel-level fusion algorithms have been developed and can be broadly classified as [7] substitution techniques, transform domain methods and optimization approaches (relying on Bayesian models, fuzzy logic and neural networks to name a few). This work employs the first two types of fusion.

Substitution techniques such as Principal Component Analysis (PCA), weighted averaging, Intensity Hue Saturation (IHS), averaging and weighted averaging are the simplest way to perform image fusion. The fused image is reconstructed by calculating the simple mean of the source images pixel-by-pixel or obtained by using the weighted averaging approach. In this method, weights are calculated

according to the neighbourhood of each pixel. However, these methods suffer from contrast degradation and artefacts in the fused images.

Transform domain techniques overcome the limitations of the substitution methods. These techniques comprise multiresolution decomposition, Wavelet Transform (WT), Laplacian Pyramid (LP), and other multidirectional transforms relying on the Contourlet Transform, and the Curvelet Transform. The LP and WT are the most well-known multiresolution approaches widely used in image fusion. In general, the Discrete Wavelet Transform (DWT) methods perform better than LP procedures [8].

The WT is exponentially proliferating in many image processing tasks, including compression, denoising, feature extraction, inverse problems, image enhancement, restoration and image fusion, because of it provides good directional information and offers a better representation in the decomposed components' domain and better results than the Pyramid Transform (PT) [9].

The Discrete Wavelet Transform (DWT) is a popular Wavelet Transform used in image fusion. DWT-based fusion methods outperform the conventional image fusion methods based on the PT, regarding a proper localization in both the spatial and the frequency domains, and the ability to capture significant information of the input image. DWT provides good spectral information and better directional information along three spatial orientations (vertical, horizontal, and diagonal) as compared to pyramid representations. Furthermore, the DWT provides other important features like excellent energy compaction by representing the entire image information using few significant coefficients and offers higher flexibility in choosing an appropriate basis function to develop new and efficient image fusion methods. Therefore, these essential properties of the DWT lead the researchers to develop DWT-based fusion algorithms for a variety of image data sets such as multi-focus images, panchromatic and multispectral satellite images, infrared and visible images.

Wavelet-based fusion methods were presented by Li et al. [10] relying on the DWT and including a maximum selection rule to determine which of the wavelet coefficients contain the relevant information, within a centred window. The major shortcoming of this method is the use of the same fusion rule for combining both approximation coefficients (low-frequency subbands) and detail coefficients (high-frequency subbands). Since the wavelet and detail coefficient have different characteristics, we have proposed two distinguished fusion rules to merge the coefficients of approximation subbands as well as the detail subbands separately.

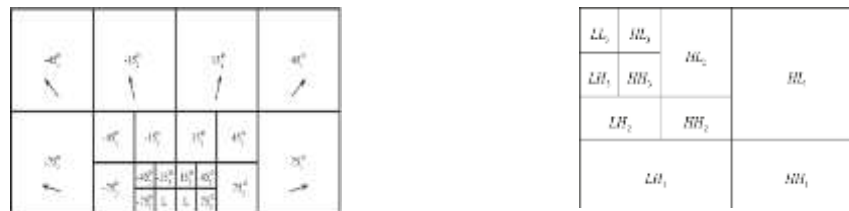
Several research works have showed that DWT suffers from shift sensitivity, the absence of phase information and poor directionality [9]. To remove out these limitations, DTCWT [11-12] inherits all the advantages of wavelet transform and provide an approximate shift invariant with better directionality than DWT, and provide perfect reconstruction using short linear-phase filters, orthogonality and symmetry properties. For these reasons, we have chosen DTCWT and incorporate two different fusion rules in our developed fusion algorithm.

### **3. The 2-D Dual-Tree Complex Wavelet Transform**

In the multi-resolution context, any function  $f \in L_2(\mathbb{R}^2)$  of size  $n \times m$  can be represented as:

$$\begin{aligned}
 & f(x, y) \\
 &= \frac{1}{\sqrt{n \times m}} \sum_k c_j^A(k) \phi_{J,K,k}(x, y) \\
 &+ \sum_{i=H,V,D} \sum_{j=1}^J \sum_k d_j^o(k) \psi_{j,K}^o(x, y)
 \end{aligned} \tag{1}$$

Where J is the largest level of decomposition and  $c_j^A$  denotes coefficients in the approximate subband in this level.  $d_j^o$  represents the detail coefficient in the level j ( $j \in 1, 2, \dots, J$ ) of orientation o ( $o \in H, V, D$ ). Here H, V and D mean the three subbands which contain detail information in the horizontal, vertical, and the diagonal directions, respectively. The 2-D scaling  $\phi(x, y)$  and the three 2-D wavelet  $\psi^o(x, y)$  functions are obtained using the product of their associated 1-D scaling and wavelet functions [12]. The proposed method uses DTCWT which is an extension of the DWT. The DTCWT, as the name implies, it consists of two trees of real filters and provides six pairs of subbands (for both the real and imaginary wavelet coefficients) using complex scaling and wavelet functions. Where the 2D DWT only separates information into horizontal, vertical and diagonal information, the 2D DTCWT separate the same information into six directional subbands, with the angles centered around  $15^\circ$ ,  $45^\circ$ ,  $75^\circ$ , and their negative equivalents as shown in Figure 1.



(a) Three levels of 2D DTCWT decomposition. (b) Three levels of 2D DWT decomposition

Figure 1. Multiresolution 2-D wavelet decomposition.

## 4. The FSPCA-DTCWT Method

As previously mentioned, the focal step in the wavelet-based image fusion techniques lies in the wavelet coefficients combination, where the main objective is to reconstruct an image with all useful information contained in the wavelet coefficients of the decomposed input images. In the present work, we have processed the approximation and detail wavelet coefficients separately using different fusion rules; this is due primarily to the different characteristics of the wavelet coefficients. The approximation coefficients (low-frequency subbands) are selected by Max-PCA fusion rule, while the detail coefficients (which correspond to the high-frequency subbands) are fused using different selection criteria to integrate the image blocks that have more information than the image blocks of the second input. The overall schematic diagram illustrating our proposed fusion method is shown in Figure 2.

### Fusion of approximation coefficients

The coefficients from the low-frequency subbands represent the approximation component, it contains most of the information and energy of input images and

introduces the visible distortions. Hence, we propose a scheme by using PCA to merge the approximation coefficients.

The primary goal of PCA is data reduction with the minimum loss of information, where the first component contains the most representative knowledge of the original data. A new fusion rule (called Max-PCA) finds the approximation coefficients of the fused image. Therefore, the process of fusing the approximation coefficients using the Max-PCA fusion rule consists of the following steps [14]:

The approximation coefficients of the two input images are arranged in two column vectors.

Computing the empirical mean along each column vector and then substrate it from the data of each column. The resulting matrix is of dimension  $2 \times n$ , where  $n$  is the length of each column vector.

Find the covariance matrix  $L$  of the resulting matrix in the previous step.

Compute the eigenvectors  $ev$  and eigenvalues  $ed$  of  $L$  and sort them by decreasing eigenvalue. Note that both  $ev$  and  $ed$  are of dimension  $2 \times 2$

Consider the first column of  $ev$  which corresponds to larger eigenvalue to compute  $P_1$  and  $P_2$ , where:  $P_1 = \frac{ev(1)}{\sum ev}$  and  $P_2 = \frac{ev(2)}{\sum ev}$ .

Finally, Max-PCA fusion rule is performed to combine approximation coefficients as follows:

$$x_f^A = Max(P_1, P_2) \times (x_1^A + x_2^A) \quad (2)$$

Where  $x_1^A$  and  $x_2^A$  denote the coefficients in the approximate subband of the decomposed input images and  $x_f^A$  indicates the fused coefficient of the approximate subband.

### **Fusion of detail coefficients**

The fusion image process should not remove any valuable information present in the source images and should preserve the detailed structures such as edges, strong texture and boundaries of the image. These details of the image are Contained in the high-frequency subbands, which are the subbands containing detail coefficients. Hence, it is imperative to find the appropriate fusion rule to select the desirable detailed components of the source images. Conventional methods do not contemplate the neighbouring coefficients, while a significant correlation exists between the local neighbouring coefficients of the two source images. We have proposed a region-based method to merge the detail coefficients in the decomposition levels. This technique involves the computation of statistical features such as the standard deviation, spatial frequency and entropy of the detailed coefficients within a local neighbourhood for the decomposed source images A and B. This is mainly used to weight the contribution of the pixel centred in that region.

#### **1. Standard deviation [8]**

Standard Deviation (STD) of pixels in a neighbourhood can indicate the degree of variability of pixel values in that region. The fused coefficients of the detail subbands have a direct effect on clarity and distortion of the fused image. Standard deviation of an  $M \times N$  image is given by:

$$\sigma = \left( \frac{1}{M \times N} \sum_{m=1}^M \sum_{n=1}^N (f(m, n) - \mu)^2 \right)^2 \quad (3)$$

Where  $f(n, m)$  the pixel is value and  $\mu$  is the mean value of the image. Higher value of standard deviation indicates high quality fused image.

## 2. Spatial frequency [5]

The spatial frequency (SF) of a pixel's neighbour calculate the frequency changes along rows and columns of the decomposed source images, it reflects their activity level and clarity. Spatial Frequency (SF) of an  $M \times N$  image is given by:

$$SF = \sqrt{RF^2 + CF^2}, \text{ with}$$

$$RF = \frac{1}{M \times N} \sum_{m=1}^M \sum_{n=2}^N [f(m, n) - f(m, n-1)]^2, \text{ and}$$

$$CF = \frac{1}{M \times N} \sum_{m=1}^M \sum_{n=2}^N [f(m, n) - f(m-1, n)]^2, \quad (4)$$

Where RF and CF are the row and column frequencies, respectively. Higher value of SF indicates large information level in the image.

## 3. Entropy [15]

Entropy (EN) used to characterize the texture and to measure the information quantity contained in an image

$$EN = - \sum_{l=1}^L P_l \log_2 P_l \quad (5)$$

where L represents the number of grey levels and  $P_l$  is the ratio of the number of the pixels with grey value is equal to l over the total number of the image pixels. Higher entropy value images provide more information than lower entropy value images [15].

The fused coefficients of the detail subbands are selected according to the feature values of SF, STD, and EN. Given two blocks from the first and second input images (detail subband) if the first block contains better values of SF and STD than the second block, then the first block will be selected and inserted in the fused coefficients of the detail subband.

Once the fused details and approximation coefficients have been calculated, the inverse DTCWT is applied to provide the final fused image. We can summarize the FSPCA-DTCWT fusion process as follows:

Step 1. Apply DTCWT to the input images.

Step 2. For detail subbands, we divide the detail subband of the input images into several blocks with a specified size, and then we apply the feature selection rule using SF, STD, and EN to obtain the fused coefficients of the detail subbands.

Step 3. For approximation subbands, we apply the proposed Max-PCA fusion rule to obtain the estimated 2D-DTCWT coefficients of the fused image.

Step 4. Apply the inverse DTCWT to get the fused image.

Figure 2 shows the main steps of FSPCA-DTCWT algorithm.

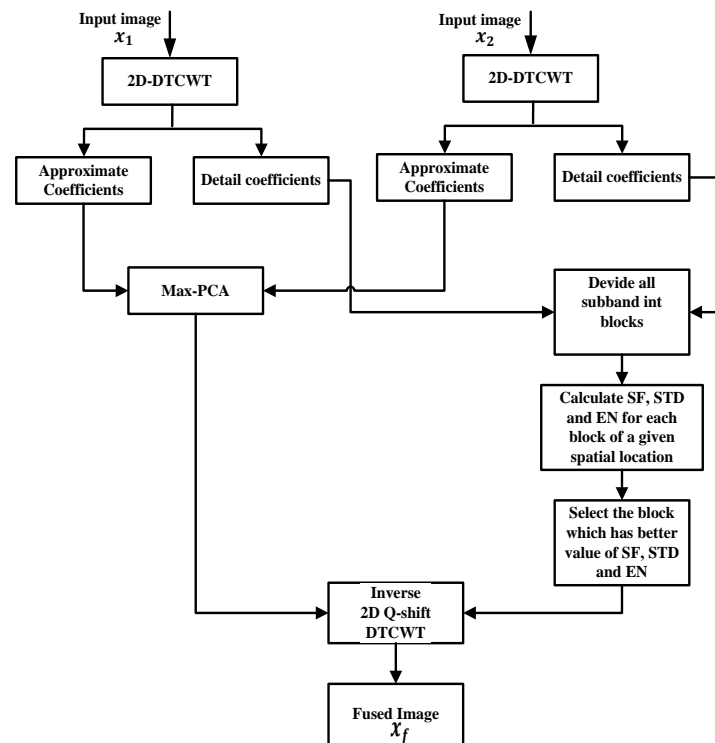


Figure 2. Schematic diagram of FSPCA-DTCWT fusion algorithm.

## 5. Experimental Results

This section analyses the performance of the FSPCA-DTCWT method. FSPCA-DTCWT has been applied to three different medical image data sets of two modalities, namely: MRI and CT images. Contrary to CT images, that provide excellent hard tissue imaging such as bones, clear and detailed images of soft tissue can be obtained from MR images. Fusion of MR and CT images integrate all possible relevant and complementary information from both MR/CT into one single image, which will be more useful for a better medical diagnosis.

The results of FSPCA-DTCWT are compared to different fusion methods in both Spatial and multiscale transform domains. This study considered the following multiscale transform methods: Morphological Pyramid (MP) [16], Discrete Wavelet Transform (DWT) [17], Discrete Cosine Harmonic Wavelet (DCHWT) [18], Spinning Sharp Frequency Localized Contourlet Transform (SFLCT\_SML) [19], and Multi-Scale Weighted Gradient-Based Fusion (MWGF) [20]. Spatial domain methods include Principal Component Analysis (PCA) [21], Cross Bilateral Filter (CBF) [22] and Bilateral Gradient-Based Sharpness Criterion (Sharp) [23].

Experiments have been conducted using Matlab 2009b with three levels of decomposition for all multiscale transform methods. Figure 3 shows the results for the first group of medical images, the latter consists of two modalities: CT image in Figure 3(a) and MR image in Figure 3(b). The desired fused image should contain both hard and soft tissue to help the medical diagnosis of pathologies.

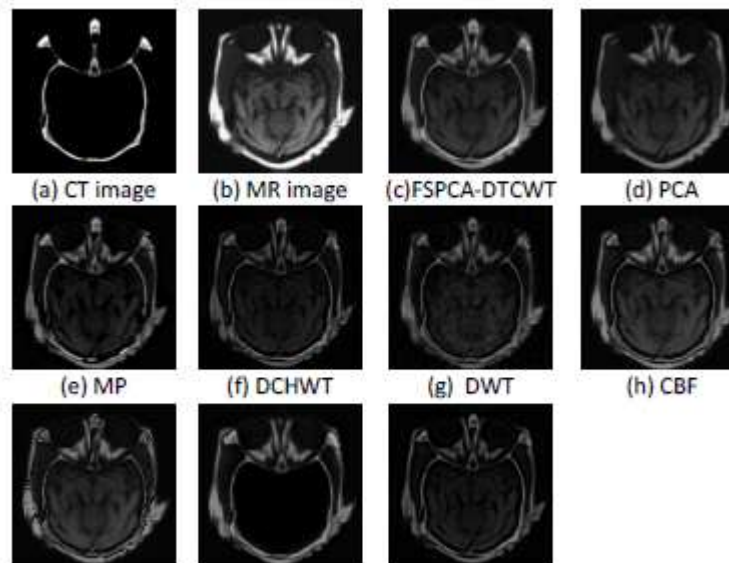


Figure 3. Image fusion results for the first set of medical images

By observing Fig.3, one can easily conclude that the fused image obtained by the proposed method Fig 3(c) provides details of bone structures as well as information about soft tissues. Nevertheless, the results of the PCA- and theMWGF-based fusion methods (Fig 3(d) and 3(j)) do not include important information contained in the first source image (Figure 3.a), while the fused images of MP-, DWT- and Sharp-based fusion methods suffer from side effects (artefacts and some deformations in different regions).

The results of the second group of images appear in Figure 4. The input images consist of T1-MR (Fig 1(a)) image that exhibits good spatial resolution and shows more evident soft tissue details and Magnetic Resonance Angiogram (MRA)(Fig 4(b)) image showing some abnormality as a calcified white structure in the image. From Figure 4, it is clear that in this case the fused image obtained by the FSPCA-DTCWT procedure keeps the highest contrast and is more informative than the fused images obtained by the other fusion methods (the PCA-, Sharp-, DWT-, CBF-, MWGF- based fusion methods).

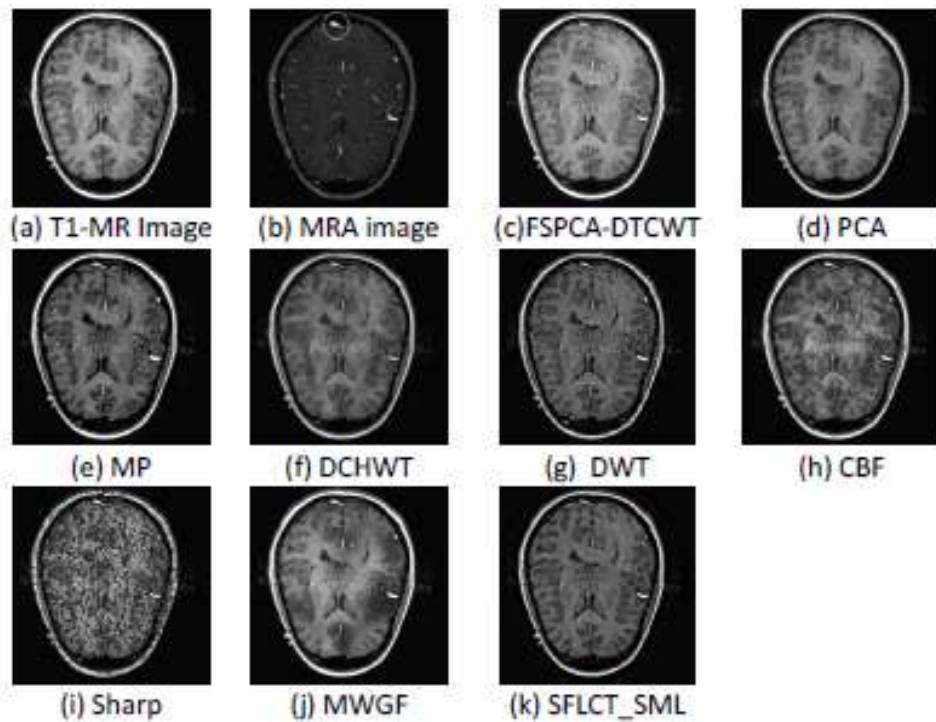


Figure 4. Image fusion results for the second set of medical images

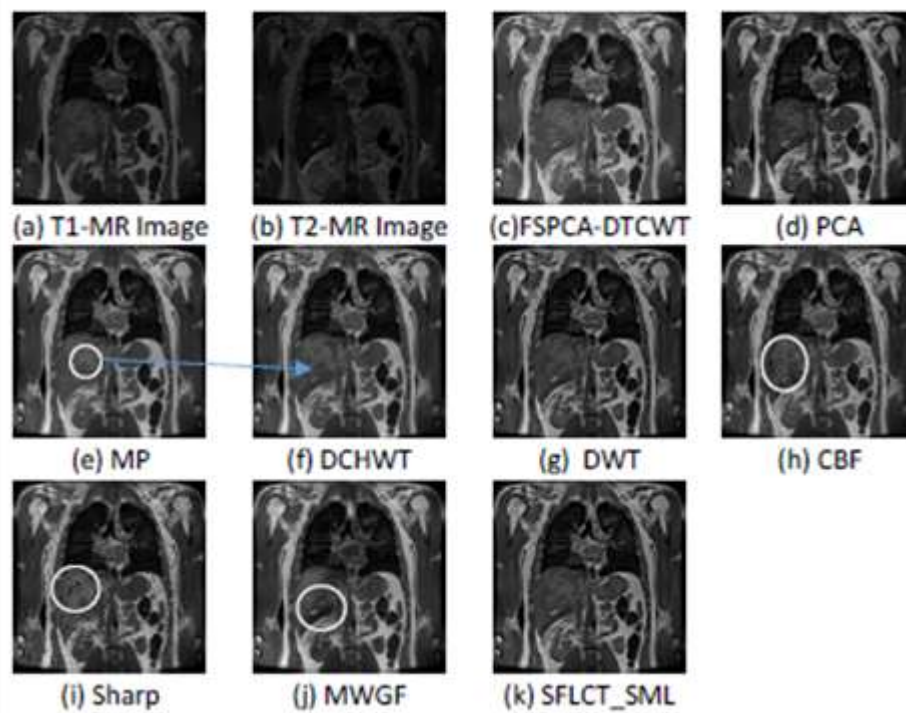


Figure 5. Image fusion results for the third set of medical images

In the third group of medical images, images a and b (Fig. 4(a)) and 4(b)) are MR-T1 and MR-T2 image, respectively. We can see that the fusion result in Fig. 4(e) obtained with MP method loses some of the information in image b. It is also clear that the fused images of CBF, Sharp and MWGF fusion methods suffer from deformations of tissue (area marked by the ellipse in Fig. 5(h-j)). The fused

images obtained by SFLC T\_SML- and DCHWT-based fusion methods have good visual

quality as the proposed method. However, the visual comparison is not sufficient to evaluate the fusion methods as in this case. Therefore, a quantitative analysis using five recent and widely used fusion performance metrics were used, namely: Standard Deviation (STD)[8], Entropy (EN)[15], Fusion Factor (FF)[8], Correlation Coefficient (CC)[24] and Visual Information Fidelity(VIF)[25].

VIF is a full reference image quality assessment metric. It is based on natural scene statistics and the notion of image information extracted by the human visual system (HVS). The quantity of visual information is considered as the amount of information extracted by the HVS from the reference image after it has passed through the distortion channel. The visual quality of the distorted image should relate to the amount of information that can be extracted by the HVS from the test image relative to the reference image information. If the amount of information that is extracted is very close to the reference image information, then the visual quality of the distorted image is very high since no loss of information occurs in the distortion channel. More details about the mathematic development of VIF can be found in [25] and [26].

FF [8] stand for the total amount of similarity between the fused image F and the source images A and B, FF is given by:

$$FF(A, B, F) = MI(A, F) + MI(B, F) \quad (6)$$

Where MI is the mutual information between source images and the fused image. Therefore, a higher value of FF shows that a larger amount of information was preserved in the fused image which indicates better fusion results. If the two images, A and F, are independent, then the mutual information similarity is zero. If the two images, A and F, are identical, all the information of A is shared with F. This performance metric can be used to help observers make quicker and more accurate decisions.

The values of the quantitative assessments for the two groups of input images (Figs. 3, 4 and Fig. 5) appear in Tables 1, 2 and 3 respectively. From table 1 and 2 (Each column's best result is shown in boldface). We can conclude that FSPCA-DTCWT algorithm outperforms the other one in terms and has better values of fusion metrics (in most of the cases). For example, the PCA- and Sharp-based fusion methods have the best values of FF (Table 1), but the visual quality of these result show a poor quality and one can observe that the corresponding fused images suffer from loss information and presence of new patterns that do not exist in any of the sources images. Similarly, the DCHWT-and Sharp-based fusion methods have the highest values of EN and FF (Table 2). However, the visual results in (Fig.4 i and f) indicate that the fused image obtained by the DCHWT-based fusion method has poor contrast as compared with that yielded with the FSPCA-DTCWT algorithm, while the fused image obtained by Sharp-based fusion method failed in preserving all relevant structures and loss of important visual information.

Table 1. Performance comparison for the first group of medical images.

Methods	STD	EN	FF	VIF	CC
FSPCA-DTCWT	<b>34.5447</b>	<b>6.1646</b>	2.8968	<b>0.6229</b>	<b>0.7081</b>
PCA	28.3806	5.6220	<b>5.2781</b>	0.2843	0.50508
MP	29.2381	5.5794	1.9303	0.4380	0.6558
DWT	22.0508	5.4541	2.1945	0.3313	0.6953
DCHWT	23.3187	5.7434	1.7824	0.3558	0.6761
CBF	30.6469	5.9157	2.8944	0.4438	0.6329
Sharp	30.9918	5.8097	5.5296	0.3501	0.5817
MWGF	33.2277	5.0722	2.1105	0.4569	0.6737
SFLCT_SML	22.5327	5.4948	1.9197	0.3539	0.6912

Table 2. Performance comparison for the second group of medical images.

Methods	STD	EN	FF	VIF	CC
FSPCA-TCWT	<b>67.2241</b>	<b>6.0301</b>	4.2017	<b>0.8684</b>	<b>0.9127</b>
PCA	56.5746	5.7044	5.2143	0.7448	0.9016
MP	54.5920	5.8559	3.9943	0.7721	0.8781
DWT	49.0719	5.8477	3.5730	0.5953	0.9027
DCHWT	50.4815	6.2555	3.5623	0.6693	0.9108
CBF	55.5992	5.8597	3.9321	0.7176	0.8836
Sharp	58.9186	5.8815	<b>6.4834</b>	0.4754	0.7757
MWGF	61.4758	5.8911	4.4029	0.8192	0.8860
SFLCT_SML	50.4341	5.7974	3.5792	0.6818	0.8962

Table 3. Performance comparison for the third group of medical images.

Methods	<i>STD</i>	<i>EN</i>	<i>FF</i>	<i>VIF</i>	<i>CC</i>
FSPCA-DTCWT	<b>28.7078</b>	<b>6.6174</b>	4.0653	0.9199	0.9264
PCA	23.6914	6.3015	4.7015	0.6890	0.9216
MP	28.6009	6.4188	3.5305	<b>0.9439</b>	0.9108
DWT	24.0218	6.2701	3.3806	0.6827	0.9187
DCHWT	23.6866	6.2919	3.1834	0.6664	0.9147
CBF	23.4422	6.2859	4.0970	0.6845	<b>0.9269</b>
Sharp	25.8353	6.4203	3.9854	0.7660	0.9097
MWGF	28.7378	6.4916	5.7157	0.8795	0.8950
SFLCT_SML	28.2195	6.5126	<b>6.7962</b>	0.7629	0.8592

Similarly, the results in Table 5 give the advantage to FSPCA-DTCWT algorithm with respect to the different fusion methods belonging to the spatial domain and the transformation domain. SFLCT\_SML- and CBF- based fusion method have the best value of FF and CC, respectively. However, the individual comparisons of the proposed method with SFLCT\_SML and CBF have proved the superiority of the proposed method in the most cases of the evaluation criteria used in this paper. Moreover, comparison should be made on the basis of both, visually and quantitatively. For example, MP method has higher VIF value but has a poor visual quality than the proposed method and failed to capture all relevant information contained in the source images (it can be easily observed from Fig.5) From the above discussion, one can conclude that the quantitative results of the proposed method are consistent with the visual analysis results.

Through the obtained results of the qualitative evaluation and quantitative indicators, we can see that FSPCA-DTCWT algorithm is found to be better than other transform domain methods and spatial domain methods. Also, FSPCA-DTCWT algorithm is able to preserve detail information such as edges and boundaries.

## 6. Conclusion

In this paper, we have proposed a new fusion method using DTCWT which is approximately shift invariant and has the high directionality properties that improve the quality of fusion results. The major contributions of this paper are twofold. First, we used a Maximum-PCA fusion rule to merge the approximation coefficients. Second, a feature selection process is proposed to select the blocks containing the most essential information from the source images.

The experimental results show that the proposed method has better performance than both multiscale transform domain methods and spatial domain methods in the visual effects and quantitative fusion evaluation measures.

## 7. Declaration of conflicts

This paper is a revised and expanded version of a paper entitled ‘An Efficient Algorithm for Multimodal Medical Image Fusion based On Feature Selection and

PCA Using DTCWT.’ presented at the International Workshop on Medical Technologies 2017 co-located with ICHSMT2017, Tlemcen, Algeria, 10–12October 2017 [1].

## 8. Authors’ biography

**Abdallah Bengueddoudj** was born in Bordj Bou Arreridj (Algeria), on August 1988, he received the B.S. degree in electronic in 2009 and the Master degree in electrical engineering in 2011. He is currently a candidate for the Ph.D. degree in electrical engineering and industrial informatics. His research interests include biometric systems, multiresolution and wavelet analysis, pattern recognition and image processing.

**Zoubeida Messali** was born in Constantine (Algeria), on November 1972, she received the B.S. degree in electronic engineering in 1995, the Master degree in signal and image processing in 2000 and Ph.D. degree in 2007 from Constantine University, Algeria. Since 2002, she has been working as a Teaching Assistant in the Department of Electronics at Msila University, and university of Bordj Bou Arreridj, Algeria. Her research interests include distributed detection networks, multiresolution and wavelet analysis, estimation theory, and medical image processing.

## 9. REFERENCES

- [1]A. Bengueddoudj and Z. Messali, “An Efficient Algorithm for Multimodal Medical Image Fusion based On Feature Selection and PCA Using DTCWT.”, *Medical Technologies Journal*, vol. 1, no. 3, pp. 60-61, Sep. 2017.<https://doi.org/10.26415/2572-004X-vol1iss3p60-61>
- [2]A. P. James and B. V. Dasarathy, "Medical image fusion: A survey of the state of the art," *Inf. Fusion*, vol. 19, pp. 4–19, 2014. <https://doi.org/10.1016/j.inffus.2013.12.002>
- [3]D. Delbeke, R. E. Coleman, M. J. Guiberteau, M. L. Brown, H. D. Royal, B. a Siegel, D. W. Townsend, L. L. Berland, J. A. Parker, G. Zubal, and V. Cronin, "Procedure Guideline for SPECT/CT Imaging 1.0.," *J. Nucl. Med.*, vol. 47, no. 7, pp. 1227–34, Jul. 2006. PMID:16818960
- [4]Q. Wang, S. Li, H. Qin, and A. Hao, "Robust multi-modal medical image fusion via anisotropic heat diffusion guided low-rank structural analysis," *Inf. Fusion*, vol. 26, pp. 103–121, 2015. <https://doi.org/10.1016/j.inffus.2015.01.001>
- [5]P. Ganasala and V. Kumar, "CT and MR Image Fusion Scheme in Nonsampled Contourlet Transform Domain," *J. Digit. Imaging*, vol. 27, no. 3, pp. 407–418, Jun. 2014. <https://doi.org/10.1007/s10278-013-9664-x> PMID:24474580 PMID:PMC4026459
- [6]A. Saleem, A. Beghdadi, and B. Boashash, “Image fusion-based contrast enhancement,” *EURASIP J. Image Video Process.*, vol. 2012, no. 1, p. 10, 2012. <https://doi.org/10.1186/1687-5281-2012-10>
- [7]S. Daneshvar and H. Ghassemian, "MRI and PET image fusion by combining IHS and retina-inspired models," *Inf. Fusion*, vol. 11, no. 2, pp. 114–123, Apr. 2010. <https://doi.org/10.1016/j.inffus.2009.05.003>
- [8]R. Singh and A. Khare, "Fusion of multimodal medical images using Daubechies complex wavelet transform – A multiresolution approach," *Inf. Fusion*, vol. 19, pp. 49–60, Sep. 2014. <https://doi.org/10.1016/j.inffus.2012.09.005>
- [9]K. Amolins, Y. Zhang, and P. Dare, "Wavelet based image fusion techniques — An introduction, review and comparison," *ISPRS J. Photogramm. Remote Sens.*, vol. 62, no. 4, pp. 249–263, Sep. 2007. <https://doi.org/10.1016/j.isprsjprs.2007.05.009>
- [10]Li, Hui, B. S. Manjunath, and Sanjit K. Mitra, "Multisensor image fusion using the wavelet transform," *Graphical models and image processing.*, vol. 57, no. 3, pp. 235–245, 1995. <https://doi.org/10.1016/j.isprsjprs.2007.05.009>
- [11]J. W. Selesnick, R. G. Baraniuk, and N. G. Kingsbury, "The dual-tree complex wavelet transform," *IEEE Signal Process. Mag.*, vol. 22, no. 6, pp. 123–151, 2005. <https://doi.org/10.1109/MSP.2005.1550194>

- [12] G. Chen and Y. Gao, "Multisource image fusion based on double density Dual-tree Complex Wavelet transform," 2012 9th Int. Conf. Fuzzy Syst. Knowl. Discov., vol. 1, no. Fskd, pp. 1864–1868, May 2012. <https://doi.org/10.1109/FSKD.2012.6233906>
- [13] P. Ramírez-Cobo, K. S. Lee, A. Molini, A. Porporato, G. Katul, and B. Vidakovic, "A wavelet-based spectral method for extracting self-similarity measures in time-varying two-dimensional rainfall maps," *J. Time Ser. Anal.*, vol. 32, no. 4, pp. 351–363, Jul. 2011. <https://doi.org/10.1111/j.1467-9892.2011.00731.x>
- [14] A. Bengueddoudj, Z. Messali, and V. Mosorov, "A Novel Image Fusion Algorithm Based on 2D Scale-Mixing Complex Wavelet Transform and Bayesian MAP Estimation for Multimodal Medical Images," *J. Innov. Opt. Health Sci.*, vol. 10, no. 6, p. 1750001, Nov. 2016.
- [15] H. Jiang and Y. Tian, "Fuzzy image fusion based on modified Self-Generating Neural Network," *Expert Syst. Appl.*, vol. 38, no. 7, pp. 8515–8523, 2011. <https://doi.org/10.1016/j.eswa.2011.01.052>
- [16] N. Uniyal, "Image Fusion using Morphological Pyramid Consistency Method," vol. 95, no. 25, pp. 34–38, 2014. PMCid:PMC4271098
- [17] L. Chiorean and M.-F. Vaida, "Medical image fusion based on discrete wavelet transform using Java technology," in *Proceedings of the ITI 2009 31st International Conference on Information Technology Interfaces*, 2009, pp. 55–60. <https://doi.org/10.1109/ITI.2009.5196054>
- [18] B. K. Shreyamsha Kumar, "Multifocus and multispectral image fusion based on pixel significance using discrete cosine harmonic wavelet transform," *Signal, Image Video Process.*, vol. 7, no. 6, pp. 1125–1143, Nov. 2013. <https://doi.org/10.1007/s11760-012-0361-x>
- [19] Q. U. X. Y. A. N. Jing-wen and Y. Gui-de, "Sum-modified-Laplacian-based Multifocus Image Fusion Method in Cycle Spinning Sharp Frequency Localized Contourlet Transform Domain," no. 60472081.
- [20] Z. Zhou, S. Li, and B. Wang, "Multi-scale weighted gradient-based fusion for multi-focus images," *Inf. Fusion*, vol. 20, no. 1, pp. 60–72, 2014. <https://doi.org/10.1016/j.inffus.2013.11.005>
- [21] V.P.S. Naidu and J.R. Raol, "Pixel-level Image Fusion using Wavelets and Principal Component Analysis," *Def. Sci. J.*, vol. 58, no. 3, pp. 338–352, 2008. <https://doi.org/10.14429/dsj.58.1653>
- [22] B. K. Shreyamsha Kumar, "Image fusion based on pixel significance using cross bilateral filter," *Signal, Image Video Process.*, vol. 9, no. 5, pp. 1193–1204, Jul. 2015. <https://doi.org/10.1007/s11760-013-0556-9>
- [23] Tian, J., Chen, L., Ma, L., and Yu, W, "Multi-focus image fusion using a bilateral gradient-based sharpness criterion," vol. 284, no. 1, pp. 80–87, 2011. <https://doi.org/10.1016/j.optcom.2010.08.085>
- [24] J. L. Crowley and J. Martin, "Experimental comparison of correlation techniques," in *IAS-4, International Conference on Intelligent Autonomous Systems*, Karlsruhe, 1995.
- [25] H. R. Sheikh and A. C. Bovik, "Image information and visual quality," *IEEE Trans. Image Process.*, vol. 15, no. 2, pp. 430–444, 2006. <https://doi.org/10.1109/TIP.2005.859378> PMid:16479813
- [26] Han Y, Cai Y, Cao Y, Xu X. "A new image fusion performance metric based on visual information fidelity," *Inf Fusion.*, vol. 14, no. 2, pp. 127–135, 2013. <https://doi.org/10.1016/j.inffus.2011.08.002>. PMid:16479813